These reflection conditions that are not related to space-group operations are given in Chapter 2.3 only for special positions. They may arise, however, also for different reasons. For example, a heavy atom at the origin of the space group $P2_12_12_1$ would generate *F*-centring with corresponding apparent absences (*cf.* the special position 4*a* of the space group *Pbca* and the absences it generates).

We wish to point out that the most common 'special-position absence' in molecular structures is due to a heavy atom at the origin of the space group $P2_1/c$.

1.6.4. Tables of reflection conditions and possible space groups

By H. D. Flack and U. Shmueli

1.6.4.1. Introduction

The primary order of presentation of these tables of reflection conditions of space groups is the Bravais lattice. This order has been chosen because cell reduction on unit-cell dimensions leads to the Bravais lattice as described as stage 1 in Section 1.6.2.1. Within the space groups of a given Bravais lattice, the entries are arranged by Laue class, which may be obtained as described as stage 2 in Section 1.6.2.1. As a consequence of these decisions about the way the tables are structured, in the hexagonal family one finds for the Bravais lattice *hP* that the Laue classes $\overline{3}$, $\overline{3}m1$, $\overline{3}1m$, 6/*m* and 6/*mmm* are grouped together.

As an aid in the study of naturally occurring macromolecules and compounds made by enantioselective synthesis, the space groups of enantiomerically pure compounds (Sohncke space groups) are typeset in bold.

The tables show, on the left, sets of reflection conditions and, on the right, those space groups that are compatible with the given set of reflection conditions. The reflection conditions, *e.g.* h or $k + l$, are to be understood as $h = 2n$ or $k + l = 2n$, respectively. All of the space groups in each table correspond to the same Patterson symmetry, which is indicated in the table header. This makes for easy comparison with the entries for the individual space groups in Chapter 2.3 of this volume, in which the Patterson symmetry is also very clearly shown. All space groups with a conventional choice of unit cell are included in Tables 1.6.4.2–1.6.4.30. All alternative settings displayed in Chapter 2.3 are thus included. The following further alternative settings, not displayed in Chapter 2.3, are also included: space group $Pb\overline{3}$ (205) and all the space groups with an *hR* Bravais lattice in the reverse setting with hexagonal axes.

Table 1.6.2.1 gives some relevant statistics drawn from Tables 1.6.4.2–1.6.4.30. The total number of space-group settings mentioned in these tables is 416. This number is considerably larger than the 230 space-group types described in Part 2 of this volume. The following example shows why the tables include data for several descriptions of the space-group types. At the stage of space-group determination for a crystal in the crystal class *mm*2, it is not yet known whether the twofold rotation axis lies along **a**, **b** or **c**. Consequently, space groups based on the three point groups 2*mm*, *m*2*m* and *mm*2 need to be considered.

In some texts dealing with space-group determination, a 'diffraction symbol' (sometimes also called an 'extinction symbol') in the form of a Hermann–Mauguin space-group symbol is used as a shorthand code for the reflection conditions and Laue class. These symbols were introduced by Buerger (1935, 1942, 1969) and a concise description is to be found in Looijenga-Vos & Buerger (2002). Nespolo *et al.* (2014) use them.

1.6.4.2. Examples of the use of the tables

(1) If the Bravais lattice is *oI* and the Laue class is *mmm*, Table 1.6.4.1 directs us to Table 1.6.4.11. Given the observed reflection conditions

$$hkl\colon h + k + l = 2n, \quad 0kl\colon k = 2n, l = 2n, \quad h0l\colon h + l = 2n,$$
$$hk0\colon h + k = 2n, \quad h00\colon h = 2n, \quad 0k0\colon k = 2n, \quad 00l\colon l = 2n,$$

it is seen from Table 1.6.4.11 that the possible settings of the space groups are: *Ibm*2 (46), *Ic*2*m* (46), *Ibmm* (74) and *Icmm* (74).

(2) If the Bravais lattice is *oP* and the Laue class is *mmm*, Table 1.6.4.1 directs us to Table 1.6.4.7. If there are no conditions on 0*kl*, the space groups *P*222 to *Pmnn* should be searched. If the condition is 0*kl*: $k = 2n$ or $l = 2n$, the space groups *Pbm*2 to *Pcnn* should be searched. If the condition is 0*kl*: $k + l = 2n$, the space groups $Pnm2_1$ to *Pnnn* should be searched.

(3) If the Bravais lattice is *cP* and the Laue class is $m\overline{3}$, Table 1.6.4.1 directs us to Table 1.6.4.25. If the conditions are 0*kl*: $k = 2n$ and *h*00: $h = 2n$, it is readily seen that the space group is $Pa\overline{3}$.

(4) If only the Bravais lattice is known or assumed, which is the case in powder-diffraction work (see Section 1.6.5.3), all tables of this section corresponding to this Bravais lattice need to be consulted. For example, if it is known that the Bravais lattice is of type *cP*, Table 1.6.4.1 tells us that the possible Laue classes are $m\overline{3}$ and $m\overline{3}m$, and the possible space groups can be found in Tables 1.6.4.25 and 1.6.4.26, respectively. The appropriate reflection conditions are of course given in these tables. All relevant tables can thus be located with the aid of Table 1.6.4.1 if the Bravais lattice is known.

1.6.5. Specialized methods of space-group determination

By H. D. Flack

1.6.5.1. Applications of resonant scattering to symmetry determination

1.6.5.1.1. Introduction

In small-molecule crystallography, it has been customary in crystal-structure analysis to make no use of the contribution of resonant scattering (otherwise called anomalous scattering and in older literature anomalous dispersion) other than in the specific area of absolute-structure and absolute-configuration determination. One may trace the causes of this situation to the weakness of the resonant-scattering contribution, to the high cost in time and labour of collecting intensity data sets containing measurements of all Friedel opposites and for a lack of any perceived or real need for the additional information that might be obtained from the effects of resonant scattering.

On the experimental side, the turning point came with the widespread distribution of area detectors for small-molecule crystallography, giving the potential to measure, at no extra cost, full-sphere data sets leading to the intensity differences between Friedel opposites hkl and $\overline{hkl}$. In 2015, the new methods of data analysis briefly presented here are in the stage of development

(*continued on page* 125)

Table 1.6.4.1
Summary of Tables 1.6.4.2–1.6.4.30

Table No.	Bravais lattice	Laue class	Patterson symmetry	Comment
1.6.4.2	*aP*	$\bar{1}$	$P\bar{1}$	
1.6.4.3	*mP*	2/*m*	*P*12/*m*1	Unique *b*
1.6.4.4	*mS* (*mC*, *mA*, *mI*)	2/*m*	*C*12/*m*1, *A*12/*m*1, *I*12/*m*1	Unique *b*
1.6.4.5	*mP*	2/*m*	*P*112/*m*	Unique *c*
1.6.4.6	*mS* (*mA*, *mB*, *mI*)	2/*m*	*A*112/*m*, *B*112/*m*, *I*112/*m*	Unique *c*
1.6.4.7	*oP*	*mmm*	*Pmmm*	
1.6.4.8	*oS* (*oC*)	*mmm*	*Cmmm*	
1.6.4.9	*oS* (*oB*)	*mmm*	*Bmmm*	
1.6.4.10	*oS* (*oA*)	*mmm*	*Ammm*	
1.6.4.11	*oI*	*mmm*	*Immm*	
1.6.4.12	*oF*	*mmm*	*Fmmm*	
1.6.4.13	*tP*	4/*m*	*P*4/*m*	
1.6.4.14	*tP*	4/*mmm*	*P*4/*mmm*	
1.6.4.15	*tI*	4/*m*	*I*4/*m*	
1.6.4.16	*tI*	4/*mmm*	*I*4/*mmm*	
1.6.4.17	*hP*	$\bar{3}$	$P\bar{3}$	
1.6.4.18	*hP*	$\bar{3}1m$ and $\bar{3}m1$	$P\bar{3}1m$ and $P\bar{3}m1$	
1.6.4.19	*hP*	6/*m*	*P*6/*m*	
1.6.4.20	*hP*	6/*mmm*	*P*6/*mmm*	
1.6.4.21	*hR*	$\bar{3}$	$R\bar{3}$	Hexagonal axes
1.6.4.22	*hR*	$\bar{3}m$	$R\bar{3}m$	Hexagonal axes
1.6.4.23	*hR*	$\bar{3}$	$R\bar{3}$	Rhombohedral axes
1.6.4.24	*hR*	$\bar{3}m$	$R\bar{3}m$	Rhombohedral axes
1.6.4.25	*cP*	$m\bar{3}$	$Pm\bar{3}$	
1.6.4.26	*cP*	$m\bar{3}m$	$Pm\bar{3}m$	
1.6.4.27	*cI*	$m\bar{3}$	$Im\bar{3}$	
1.6.4.28	*cI*	$m\bar{3}m$	$Im\bar{3}m$	
1.6.4.29	*cF*	$m\bar{3}$	$Fm\bar{3}$	
1.6.4.30	*cF*	$m\bar{3}m$	$Fm\bar{3}m$	

Table 1.6.4.2
Reflection conditions and possible space groups with Bravais lattice *aP* and Laue class $\bar{1}$; Patterson symmetry $P\bar{1}$

Reflection conditions	Space group	No.	Space group	No.
	***P*1**	1	$P\bar{1}$	2

Table 1.6.4.3
Reflection conditions and possible space groups with Bravais lattice *mP* and Laue class 2/*m*; (monoclinic, unique axis *b*); Patterson symmetry *P*12/*m*1

Reflection conditions						Space group	No.	Space group	No.	Space group	No.
*h*0*l*	0*kl*	*hk*0	0*k*0	*h*00	00*l*						
						***P*2**	3	*Pm*	6	*P*2/*m*	10
			k			***P*2$_1$**	4	*P*2$_1$/*m*	11		
h				*h*		*Pa*	7	*P*2/*a*	13		
h			*k*	*h*		*P*2$_1$/*a*	14				
l					*l*	*Pc*	7	*P*2/*c*	13		
l			*k*		*l*	*P*2$_1$/*c*	14				
h + *l*				*h*	*l*	*Pn*	7	*P*2/*n*	13		
h + *l*			*k*	*h*	*l*	*P*2$_1$/*n*	14				

Table 1.6.4.4
Reflection conditions and possible space groups with Bravais lattice *mS* (*mC*, *mA*, *mI*) and Laue class 2/*m* (monoclinic, unique axis *b*); Patterson symmetry *C*12/*m*1, *A*12/*m*1, *I*12/*m*1

Reflection conditions							Space group	No.	Space group	No.	Space group	No.
hkl	*h*0*l*	0*kl*	*hk*0	0*k*0	*h*00	00*l*						
$h + k$	h	k	$h + k$	k	h		***C*2**	5	*Cm*	8	*C*2/*m*	12
$h + k$	h, l	k	$h + k$	k	h	l	*Cc*	9	*C*2/*c*	15		
$k + l$	l	$k + l$	k	k		l	***A*2**	5	*Am*	8	*A*2/*m*	12
$k + l$	h, l	$k + l$	k	k	h	l	*An*	9	*A*2/*n*	15		
$h + k + l$	$h + l$	$k + l$	$h + k$	k	h	l	***I*2**	5	*Im*	8	*I*2/*m*	12
$h + k + l$	h, l	$k + l$	$h + k$	k	h	l	*Ia*	9	*I*2/*a*	15		

Table 1.6.4.5
Reflection conditions and possible space groups with Bravais lattice *mP* and Laue class 2/*m* (monoclinic, unique axis *c*); Patterson symmetry *P*112/*m*

Reflection conditions						Space group	No.	Space group	No.	Space group	No.
*h*0*l*	0*kl*	*hk*0	0*k*0	*h*00	00*l*						
						***P*2**	3	*Pm*	6	*P*2/*m*	10
					l	***P*2$_1$**	4	*P*2$_1$/*m*	11		
		h		h		*Pa*	7	*P*2/*a*	13		
		h		h	l	*P*2$_1$/*a*	14				
		k	k			*Pb*	7	*P*2/*b*	13		
		k	k		l	*P*2$_1$/*b*	14				
		$h + k$	k	h		*Pn*	7	*P*2/*n*	13		
		$h + k$	k	h	l	*P*2$_1$/*n*	14				

Table 1.6.4.6
Reflection conditions and possible space groups with Bravais lattice *mS* (*mA*, *mB*, *mI*) and Laue class 2/*m* (monoclinic, unique axis *c*); Patterson symmetry *A*112/*m*, *B*112/*m*1, *I*112/*m*

Reflection conditions							Space group	No.	Space group	No.	Space group	No.
hkl	*h*0*l*	0*kl*	*hk*0	0*k*0	*h*00	00*l*						
$k + l$	l	$k + l$	k	k		l	***A*2**	5	*Am*	8	*A*2/*m*	12
$k + l$	l	$k + l$	h, k	k	h	l	*Aa*	9	*A*2/*a*	15		
$h + l$	$h + l$	l	h		h	l	***B*2**	5	*Bm*	8	*B*2/*m*	12
$h + l$	$h + l$	l	h, k	k	h	l	*Bn*	9	*B*2/*n*	15		
$h + k + l$	$h + l$	$k + l$	$h + k$	k	h	l	***I*2**	5	*Im*	8	*I*2/*m*	12
$h + k + l$	$h + l$	$k + l$	h, k	k	h	l	*Ib*	9	*I*2/*b*	15		

Table 1.6.4.7
Reflection conditions and possible space groups with Bravais lattice *oP* and Laue class *mmm*; Patterson symmetry *Pmmm*

Reflection conditions						Space group	No.	Space group	No.	Space group	No.
0*kl*	*h*0*l*	*hk*0	*h*00	0*k*0	00*l*						
						***P*222** *P*2*mm*	16 25	*Pmm*2 *Pmmm*	25 47	*Pm*2*m*	25
					l	***P*222$_1$**	17				
				k		***P*22$_1$2**	17				
				k	*l*	***P*22$_1$2$_1$**	18				
			h			***P*2$_1$22**	17				
			h		*l*	***P*2$_1$22$_1$**	18				
			h	*k*		***P*2$_1$2$_1$2**	18				
			h	*k*	*l*	***P*2$_1$2$_1$2$_1$**	19				
		h	*h*			*P*2$_1$*ma*	26	*Pm*2*a*	28	*Pmma*	51
		k		*k*		*Pm*2$_1$*b*	26	*P*2*mb*	28	*Pmmb*	51
		h + *k*	*h*	*k*		*Pm*2$_1$*n*	31	*P*2$_1$*mn*	31	*Pmmn*	59
	h		*h*			*P*2$_1$*am*	26	*Pma*2	28	*Pmam*	51
	h	*h*	*h*			*P*2*aa*	27	*Pmaa*	49		
	h	*k*	*h*	*k*		*P*2$_1$*ab*	29	*Pmab*	57		
	h	*h* + *k*	*h*	*k*		*P*2*an*	30	*Pman*	53		
	l				*l*	*Pmc*2$_1$	26	*P*2*cm*	28	*Pmcm*	51
	l	*h*	*h*		*l*	*P*2$_1$*ca*	29	*Pmca*	57		
	l	*k*		*k*	*l*	*P*2*cb*	32	*Pmcb*	55		
	l	*h* + *k*	*h*	*k*	*l*	*P*2$_1$*cn*	33	*Pmcn*	62		
	h + *l*		*h*		*l*	*Pmn*2$_1$	31	*P*2$_1$*nm*	31	*Pmnm*	59
	h + *l*	*h*	*h*		*l*	*P*2*na*	30	*Pmna*	53		
	h + *l*	*k*	*h*	*k*	*l*	*P*2$_1$*nb*	33	*Pmnb*	62		
	h + *l*	*h* + *k*	*h*	*k*	*l*	*P*2*nn*	34	*Pmnn*	58		
k				*k*		*Pb*2$_1$*m*	26	*Pbm*2	28	*Pbmm*	51
k		*h*	*h*	*k*		*Pb*2$_1$*a*	29	*Pbma*	57		
k		*k*		*k*		*Pb*2*b*	27	*Pbmb*	49		
k		*h* + *k*	*h*	*k*		*Pb*2*n*	30	*Pbmn*	53		
k	*h*		*h*	*k*		*Pba*2	32	*Pbam*	55		
k	*h*	*h*	*h*	*k*		*Pbaa*	54				
k	*h*	*k*	*h*	*k*		*Pbab*	54				
k	*h*	*h* + *k*	*h*	*k*		*Pban*	50				
k	*l*			*k*	*l*	*Pbc*2$_1$	29	*Pbcm*	57		
k	*l*	*h*	*h*	*k*	*l*	*Pbca*	61				
k	*l*	*k*		*k*	*l*	*Pbcb*	54				
k	*l*	*h* + *k*	*h*	*k*	*l*	*Pbcn*	60				

Table 1.6.4.7 (continued)

Reflection conditions						Space group	No.	Space group	No.	Space group	No.
0*kl*	*h*0*l*	*hk*0	*h*00	0*k*0	00*l*						
k	*h* + *l*		*h*	*k*	*l*	*Pbn*2_1	33	*Pbnm*	62		
k	*h* + *l*	*h*	*h*	*k*	*l*	*Pbna*	60				
k	*h* + *l*	*k*	*h*	*k*	*l*	*Pbnb*	56				
k	*h* + *l*	*h* + *k*	*h*	*k*	*l*	*Pbnn*	52				
l					*l*	*Pcm*2_1	26	*Pc*2*m*	28	*Pcmm*	51
l		*h*	*h*		*l*	*Pc*2*a*	32	*Pcma*	55		
l		*k*		*k*	*l*	*Pc*2_1*b*	29	*Pcmb*	57		
l		*h* + *k*	*h*	*k*	*l*	*Pc*2_1*n*	33	*Pcmn*	62		
l	*h*		*h*		*l*	*Pca*2_1	29	*Pcam*	57		
l	*h*	*h*	*h*		*l*	*Pcaa*	54				
l	*h*	*k*	*h*	*k*	*l*	*Pcab*	61				
l	*h*	*h* + *k*	*h*	*k*	*l*	*Pcan*	60				
l	*l*				*l*	*Pcc*2	27	*Pccm*	49		
l	*l*	*h*	*h*		*l*	*Pcca*	54				
l	*l*	*k*		*k*	*l*	*Pccb*	54				
l	*l*	*h* + *k*	*h*	*k*	*l*	*Pccn*	56				
l	*h* + *l*		*h*		*l*	*Pcn*2	30	*Pcnm*	53		
l	*h* + *l*	*h*	*h*		*l*	*Pcna*	50				
l	*h* + *l*	*k*	*h*	*k*	*l*	*Pcnb*	60				
l	*h* + *l*	*h* + *k*	*h*	*k*	*l*	*Pcnn*	52				
k + *l*				*k*	*l*	*Pnm*2_1	31	*Pn*2_1*m*	31	*Pnmm*	59
k + *l*		*h*	*h*	*k*	*l*	*Pn*2_1*a*	33	*Pnma*	62		
k + *l*		*k*		*k*	*l*	*Pn*2*b*	30	*Pnmb*	53		
k + *l*		*h* + *k*	*h*	*k*	*l*	*Pn*2*n*	34	*Pnmn*	58		
k + *l*	*h*		*h*	*k*	*l*	*Pna*2_1	33	*Pnam*	62		
k + *l*	*h*	*h*	*h*	*k*	*l*	*Pnaa*	56				
k + *l*	*h*	*k*	*h*	*k*	*l*	*Pnab*	60				
k + *l*	*h*	*h* + *k*	*h*	*k*	*l*	*Pnan*	52				
k + *l*	*l*			*k*	*l*	*Pnc*2	30	*Pncm*	53		
k + *l*	*l*	*h*	*h*	*k*	*l*	*Pnca*	60				
k + *l*	*l*	*k*		*k*	*l*	*Pncb*	50				
k + *l*	*l*	*h* + *k*	*h*	*k*	*l*	*Pncn*	52				
k + *l*	*h* + *l*		*h*	*k*	*l*	*Pnn*2	34	*Pnnm*	58		
k + *l*	*h* + *l*	*h*	*h*	*k*	*l*	*Pnna*	52				
k + *l*	*h* + *l*	*k*	*h*	*k*	*l*	*Pnnb*	52				
k + *l*	*h* + *l*	*h* + *k*	*h*	*k*	*l*	*Pnnn*	48				

Table 1.6.4.8
Reflection conditions and possible space groups with Bravais lattice *oS* (*oC* setting) and Laue class *mmm*; Patterson symmetry *Cmmm*

Reflection conditions							Space group	No.	Space group	No.	Space group	No.
hkl	0*kl*	*h*0*l*	*hk*0	*h*00	0*k*0	00*l*						
$h + k$	k	h	$h + k$	h	k		***C*222** *C*2*mm*	21 38	*Cmm*2 *Cmmm*	35 65	*Cm*2*m*	38
$h + k$	k	h	$h + k$	h	k	l	***C*222$_1$**	20				
$h + k$	k	h	h, k	h	k		*Cm*2*e*	39	*C*2*me*	39	*Cme*	67
$h + k$	k	h, l	$h + k$	h	k	l	*Cmc*2$_1$	36	*C*2*cm*	40	*Cmcm*	63
$h + k$	k	h, l	h, k	h	k	l	*C*2*ce*	41	*Cmce*	64		
$h + k$	k, l	h	$h + k$	h	k	l	*Ccm*2$_1$	36	*Cc*2*m*	40	*Ccmm*	63
$h + k$	k, l	h	h, k	h	k	l	*Cc*2*e*	41	*Ccme*	64		
$h + k$	k, l	h, l	$h + k$	h	k	l	*Ccc*2	37	*Cccm*	66		
$h + k$	k, l	h, l	h, k	h	k	l	*Ccce*	68				

Table 1.6.4.9
Reflection conditions and possible space groups with Bravais lattice *oS* (*oB* setting) and Laue class *mmm*; Patterson symmetry *Bmmm*

Reflection conditions							Space group	No.	Space group	No.	Space group	No.
hkl	0*kl*	*h*0*l*	*hk*0	*h*00	0*k*0	00*l*						
$h + l$	l	$h + l$	h	h		l	***B*222** *B*2*mm*	21 38	*Bm*2*m* *Bmmm*	35 65	*Bmm*2	38
$h + l$	l	$h + l$	h	h	k	l	***B*22$_1$2**	20				
$h + l$	l	$h + l$	h, k	h	k	l	*Bm*2$_1$*b*	36	*B*2*mb*	40	*Bmmb*	63
$h + l$	l	h, l	h	h		l	*Bme*2	39	*B*2*em*	39	*Bmem*	67
$h + l$	l	h, l	h, k	h	k	l	*B*2*eb*	41	*Bmeb*	64		
$h + l$	k, l	$h + l$	h	h	k	l	*Bb*2$_1$*m*	36	*Bbm*2	40	*Bbmm*	63
$h + l$	k, l	$h + l$	h, k	h	k	l	*Bb*2*b*	37	*Bbmb*	66		
$h + l$	k, l	h, l	h	h	k	l	*Bbe*2	41	*Bbem*	64		
$h + l$	k, l	h, l	h, k	h	k	l	*Bbeb*	68				

Table 1.6.4.10
Reflection conditions and possible space groups with Bravais lattice *oS* (*oA* setting) and Laue class *mmm*; Patterson symmetry *Ammm*

Reflection conditions							Space group	No.	Space group	No.	Space group	No.
hkl	0*kl*	*h*0*l*	*hk*0	*h*00	0*k*0	00*l*						
$k + l$	$k + l$	l	k		k	l	***A*222** *Amm*2	21 38	*A*2*mm* *Ammm*	35 65	*Am*2*m*	38
$k + l$	$k + l$	l	k	h	k	l	***A*2$_1$22**	20				
$k + l$	$k + l$	l	h, k	h	k	l	*A*2$_1$*ma*	36	*Am*2*a*	40	*Amma*	63
$k + l$	$k + l$	h, l	k	h	k	l	*A*2$_1$*am*	36	*Ama*2	40	*Amam*	63
$k + l$	$k + l$	h, l	h, k	h	k	l	*A*2*aa*	37	*Amaa*	66		
$k + l$	k, l	l	k		k	l	*Aem*2	39	*Ae*2*m*	39	*Aemm*	67
$k + l$	k, l	l	h, k	h	k	l	*Ae*2*a*	41	*Aema*	64		
$k + l$	k, l	h, l	k	h	k	l	*Aea*2	41	*Aeam*	64		
$k + l$	k, l	h, l	h, k	h	k	l	*Aeaa*	68				

Table 1.6.4.11
Reflection conditions and possible space groups with Bravais lattice *oI* and Laue class *mmm*; Patterson symmetry *Immm*

Reflection conditions							Space group	No.	Space group	No.	Space group	No.
hkl	0*kl*	*h*0*l*	*hk*0	*h*00	0*k*0	00*l*						
$h+k+l$	$k+l$	$h+l$	$h+k$	h	k	l	***I*222** *Im*2*m*	23 44	$\boldsymbol{I2_12_12_1}$ *I*2*mm*	24 44	*Imm*2 *Immm*	44 71
$h+k+l$	$k+l$	$h+l$	h, k	h	k	l	*Im*2*a* *Immb*	46 74	*I*2*mb*	46	*Imma*	74
$h+k+l$	$k+l$	h, l	$h+k$	h	k	l	*Ima*2 *Imcm*	46 74	*I*2*cm*	46	*Imam*	74
$h+k+l$	$k+l$	h, l	h, k	h	k	l	*I*2*cb*	45	*Imcb*	72		
$h+k+l$	k, l	$h+l$	$h+k$	h	k	l	*Ibm*2 *Icmm*	46 74	*Ic*2*m*	46	*Ibmm*	74
$h+k+l$	k, l	$h+l$	h, k	h	k	l	*Ic*2*a*	45	*Icma*	72		
$h+k+l$	k, l	h, l	$h+k$	h	k	l	*Iba*2	45	*Ibam*	72		
$h+k+l$	k, l	h, l	h, k	h	k	l	*Ibca*	73	*Icab*	73		

Table 1.6.4.12
Reflection conditions and possible space groups with Bravais lattice *oF* and Laue class *mmm*; Patterson symmetry *Fmmm*

Reflection conditions							Space group	No.
hkl	0*kl*	*h*0*l*	*hk*0	*h*00	0*k*0	00*l*		
$h+k, h+l, k+l$	k, l	h, l	h, k	h	k	l	***F*222** *Fmm*2 *Fm*2*m* *F*2*mm* *Fmmm*	22 42 42 42 69
$h+k, h+l, k+l$	k, l	$h+l=4n; h, l$	$h+k=4n; h, k$	$h=4n$	$k=4n$	$l=4n$	*F*2*dd*	43
$h+k, h+l, k+l$	$k+l=4n; k, l$	h, l	$h+k=4n; h, k$	$h=4n$	$k=4n$	$l=4n$	*Fd*2*d*	43
$h+k, h+l, k+l$	$k+l=4n; k, l$	$h+l=4n; h, l$	h, k	$h=4n$	$k=4n$	$l=4n$	*Fdd*2	43
$h+k, h+l, k+l$	$k+l=4n; k, l$	$h+l=4n; h, l$	$h+k=4n; h, k$	$h=4n$	$k=4n$	$l=4n$	*Fddd*	70

Table 1.6.4.13
Reflection conditions and possible space groups with Bravais lattice *tP* and Laue class 4/*m*; *hk* are permutable; Patterson symmetry *P*4/*m*

Reflection conditions					Space group	No.	Space group	No.	Space group	No.
*hk*0	0*kl*	$h \pm h\, l$	00*l*	*h*00						
					***P*4**	75	$P\bar{4}$	81	$P4/m$	83
			l		$\boldsymbol{P4_2}$	77	$P4_2/m$	84		
			$l=4n$		$\boldsymbol{P4_1}$	76	$\boldsymbol{P4_3}$	78		
$h+k$				h	$P4/n$	85				
$h+k$			l	h	$P4_2/n$	86				

Table 1.6.4.14
Reflection conditions and possible space groups with Bravais lattice *tP* and Laue class 4/*mmm*; *hk* are permutable; Patterson symmetry *P*4/*mmm*

Reflection conditions					Space group	No.	Space group	No.	Space group	No.
*hk*0	0*kl*	*h* ± *h l*	00*l*	*h*00						
					***P*422**	89	*P*4*mm*	99	$P\bar{4}2m$	111
					$P\bar{4}m2$	115	*P*4/*mmm*	123		
				h	***P*42$_1$2**	90	$P\bar{4}2_1m$	113		
			l		***P*4$_2$22**	93				
			l	*h*	***P*4$_2$2$_1$2**	94				
			l = 4*n*		***P*4$_1$22**	91	***P*4$_3$22**	95		
			l = 4*n*	*h*	***P*4$_1$2$_1$2**	92	***P*4$_3$2$_1$2**	96		
		l	*l*		*P*4$_2$*mc*	105	$P\bar{4}2c$	112	*P*4$_2$/*mmc*	131
		l	*l*	*h*	$P\bar{4}2_1c$	114				
	k			*h*	*P*4*bm*	100	$P\bar{4}b2$	117	*P*4/*mbm*	127
	k	*l*	*l*	*h*	*P*4$_2$*bc*	106	*P*4$_2$/*mbc*	135		
	l		*l*		*P*4$_2$*cm*	101	$P\bar{4}c2$	116	*P*4$_2$/*mcm*	132
	l	*l*	*l*		*P*4*cc*	103	*P*4/*mcc*	124		
	k + *l*		*l*	*h*	*P*4$_2$*nm*	102	$P\bar{4}n2$	118	*P*4$_2$/*mnm*	136
	k + *l*	*l*	*l*	*h*	*P*4*nc*	104	*P*4/*mnc*	128		
h + *k*				*h*	*P*4/*nmm*	129				
h + *k*		*l*	*l*	*h*	*P*4$_2$/*nmc*	137				
h + *k*	*k*			*h*	*P*4/*nbm*	125				
h + *k*	*k*	*l*	*l*	*h*	*P*4$_2$/*nbc*	133				
h + *k*	*l*		*l*	*h*	*P*4$_2$/*ncm*	138				
h + *k*	*l*	*l*	*l*	*h*	*P*4/*ncc*	130				
h + *k*	*k* + *l*		*l*	*h*	*P*4$_2$/*nnm*	134				
h + *k*	*k* + *l*	*l*	*l*	*h*	*P*4/*nnc*	126				

Table 1.6.4.15
Reflection conditions and possible space groups with Bravais lattice *tI* and Laue class 4/*m*; *hk* are permutable; Patterson symmetry *I*4/*m*

Reflection conditions							Space group	No.	Space group	No.	Space group	No.
hkl	*hk*0	0*kl*	*h* ± *h l*	00*l*	*h*00	*h* ± *h* 0						
h + *k* + *l*	*h* + *k*	*k* + *l*	*l*	*l*	*h*		***I*4**	79	$I\bar{4}$	82	*I*4/*m*	87
h + *k* + *l*	*h* + *k*	*k* + *l*	*l*	*l* = 4*n*	*h*		***I*4$_1$**	80				
h + *k* + *l*	*h*, *k*	*k* + *l*	*l*	*l* = 4*n*	*h*	*h*	*I*4$_1$/*a*	88				

Table 1.6.4.16
Reflection conditions and possible space groups with Bravais lattice *tI* and Laue class 4/*mmm*; *hk* are permutable; Patterson symmetry *I*4/*mmm*

Reflection conditions							Space group	No.	Space group	No.	Space group	No.
hkl	*hk*0	0*kl*	$h \pm h\, l$	00*l*	*h*00	$h \pm h\, 0$						
$h+k+l$	$h+k$	$k+l$	l	l	h		**I422** $I\bar{4}2m$	97 121	$I4mm$ $I4/mmm$	107 139	$I\bar{4}m2$	119
$h+k+l$	$h+k$	$k+l$	l	$l=4n$	h		$\mathbf{I4_122}$	98				
$h+k+l$	$h+k$	$k+l$	$2h+l=4n$	$l=4n$	h	h	$I4_1md$	109	$I\bar{4}2d$	122		
$h+k+l$	$h+k$	k, l	l	l	h		$I4cm$	108	$I\bar{4}c2$	120	$I4/mcm$	140
$h+k+l$	$h+k$	k, l	$2h+l=4n$	$l=4n$	h	h	$I4_1cd$	110				
$h+k+l$	h, k	$k+l$	$2h+l=4n$	$l=4n$	h	h	$I4_1/amd$	141				
$h+k+l$	h, k	k, l	$2h+l=4n$	$l=4n$	h	h	$I4_1/acd$	142				

Table 1.6.4.17
Reflection conditions and possible space groups with Bravais lattice *hP* and Laue class $\bar{3}$; *hki* are permutable; Patterson symmetry $P\bar{3}$

Reflection conditions			Space group	No.	Space group	No.
$hh\bar{2}hl$	$h\bar{h}0l$	000*l*				
			P3	143	$P\bar{3}$	147
		$l=3n$	$\mathbf{P3_1}$	144	$\mathbf{P3_2}$	145

Table 1.6.4.18
Reflection conditions and possible space groups with Bravais lattice *hP* and Laue classes $\bar{3}1m$ and $\bar{3}m1$; *hki* are permutable; Patterson symmetry $P\bar{3}1m$ and $P\bar{3}m1$

Reflection conditions			Class $\bar{3}1m$		Class $\bar{3}m1$	
$hh\bar{2}hl$	$h\bar{h}0l$	000*l*	Space group	No.	Space group	No.
			P312	149	**P321**	150
			$P31m$	157	$P3m1$	156
			$P\bar{3}1m$	162	$P\bar{3}m1$	164
		$l=3n$	$\mathbf{P3_112}$	151	$\mathbf{P3_121}$	152
			$\mathbf{P3_212}$	153	$\mathbf{P3_221}$	154
l		l	$P31c$	159		
			$P\bar{3}1c$	163		
	l	l			$P3c1$	158
					$P\bar{3}c1$	165

Table 1.6.4.19
Reflection conditions and possible space groups with Bravais lattice *hP* and Laue class 6/*m*; *hki* are permutable; Patterson symmetry *P*6/*m*

Reflection conditions			Space group	No.	Space group	No.	Space group	No.
$hh\bar{2}hl$	$h\bar{h}0l$	000*l*						
			P6	168	$P\bar{6}$	174	$P6/m$	175
		l	$\mathbf{P6_3}$	173	$P6_3/m$	176		
		$l=3n$	$\mathbf{P6_2}$	171	$\mathbf{P6_4}$	172		
		$l=6n$	$\mathbf{P6_1}$	169	$\mathbf{P6_5}$	170		

Table 1.6.4.20
Reflection conditions and possible space groups with Bravais lattice *hP* and Laue class 6/*mmm*; *hki* are permutable; Patterson symmetry *P*6/*mmm*

Reflection conditions			Space group	No.	Space group	No.	Space group	No.
$hh\bar{2}\bar{h}l$	$h\bar{h}0l$	$000l$						
			***P*622**	177	*P*6*mm*	183	$P\bar{6}m2$	187
			$P\bar{6}2m$	189	*P*6/*mmm*	191		
		l	$\boldsymbol{P6_322}$	182				
		$l = 3n$	$\boldsymbol{P6_222}$	180	$\boldsymbol{P6_422}$	181		
		$l = 6n$	$\boldsymbol{P6_122}$	178	$\boldsymbol{P6_522}$	179		
l		l	$P6_3mc$	186	$P\bar{6}2c$	190	$P6_3/mmc$	194
	l	l	$P6_3cm$	185	$P\bar{6}c2$	188	$P6_3/mcm$	193
l	l	l	*P*6*cc*	184	*P*6/*mcc*	192		

Table 1.6.4.21
Reflection conditions and possible space groups with Bravais lattice *hR* and Laue class $\bar{3}$ (hexagonal axes); *hki* are permutable; Patterson symmetry $R\bar{3}$; Ov = obverse setting; Rv = reverse setting

Reflection conditions						Space group	No.	Space group	No.	
hkil	*hki*0	$hh\bar{2}\bar{h}l$	$h\bar{h}0l$	$000l$	$h\bar{h}00$					
$-h+k+l=3n$	$-h+k=3n$	$l=3n$	$h+l=3n$	$l=3n$	$h=3n$	***R*3**	146	$R\bar{3}$	148	Ov
$h-k+l=3n$	$h-k=3n$	$l=3n$	$-h+l=3n$	$l=3n$	$h=3n$	***R*3**	146	$R\bar{3}$	148	Rv

Table 1.6.4.22
Reflection conditions and possible space groups with Bravais lattice *hR* and Laue class $\bar{3}m$ (hexagonal axes); *hki* are permutable; Patterson symmetry $R\bar{3}m$; Ov = obverse setting; Rv = reverse setting

Reflection conditions						Space group	No.	Space group	No.	Space group	No.	
hkil	*hki*0	$hh\bar{2}\bar{h}l$	$h\bar{h}0l$	$000l$	$h\bar{h}00$							
$-h+k+l=3n$	$-h+k=3n$	$l=3n$	$h+l=3n$	$l=3n$	$h=3n$	***R*32**	155	*R*3*m*	160	$R\bar{3}m$	166	Ov
$-h+k+l=3n$	$-h+k=3n$	$l=3n$	$h+l=3n, l=2m$	$l=6n$	$h=3n$	*R*3*c*	161	$R\bar{3}c$	167			Ov
$h-k+l=3n$	$h-k=3n$	$l=3n$	$-h+l=3n$	$l=3n$	$h=3n$	***R*32**	155	*R*3*m*	160	$R\bar{3}m$	166	Rv
$h-k+l=3n$	$h-k=3n$	$l=3n$	$-h+l=3n, l=2m$	$l=6n$	$h=3n$	*R*3*c*	161	$R\bar{3}c$	167			Rv

Table 1.6.4.23
Reflection conditions and possible space groups with Bravais lattice *hR* and Laue class $\bar{3}$ (rhombohedral axes); *hkl* are permutable; Patterson symmetry $R\bar{3}$

Reflection conditions		Space group	No.	Space group	No.
hhl	*hhh*				
		***R*3**	146	$R\bar{3}$	148

Table 1.6.4.24
Reflection conditions and possible space groups with Bravais lattice *hR* and Laue class $\bar{3}m$ (rhombohedral axes); *hkl* are permutable; Patterson symmetry $R\bar{3}m$

Reflection conditions		Space group	No.	Space group	No.	Space group	No.
hhl	*hhh*						
		***R*32**	155	*R*3*m*	160	$R\bar{3}m$	166
l	h	*R*3*c*	161	$R\bar{3}c$	167		

Table 1.6.4.25
Reflection conditions and possible space groups with Bravais lattice *cP* and Laue class $m\bar{3}$; *hkl* are cyclically permutable; Patterson symmetry $Pm\bar{3}$

Reflection conditions			Space group	No.	Space group	No.
$0kl$	$h \pm h\,l$	$h00$				
			***P*23**	195	$Pm\bar{3}$	200
		h	***P*2$_1$3**	198		
k		h	$Pa\bar{3}$	205		
l		h	$Pb\bar{3}$	205		
$k + l$		h	$Pn\bar{3}$	201		

Table 1.6.4.26
Reflection conditions and possible space groups with Bravais lattice *cP* and Laue class $m\bar{3}m$; *hkl* are permutable; Patterson symmetry $Pm\bar{3}m$

Reflection conditions			Space group	No.	Space group	No.	Space group	No.
$0kl$	$h \pm h\,l$	$h00$						
			***P*432**	207	$P\bar{4}3m$	215	$Pm\bar{3}m$	221
		h	***P*4$_2$32**	208				
		$h = 4n$	***P*4$_3$32**	212	***P*4$_1$32**	213		
	l	h	$P\bar{4}3n$	218	$Pm\bar{3}n$	223		
$k + l$		h	$Pn\bar{3}m$	224				
$k + l$	l	h	$Pn\bar{3}n$	222				

Table 1.6.4.27
Reflection conditions and possible space groups with Bravais lattice *cI* and Laue class $m\bar{3}$; *hkl* are cyclically permutable; Patterson symmetry $Im\bar{3}$

Reflection conditions				Space group	No.	Space group	No.	Space group	No.
hkl	$0kl$	$h \pm h\,l$	$h00$						
$h + k + l$	$k + l$	l	h	***I*23**	197	***I*2$_1$3**	199	$Im\bar{3}$	204
$h + k + l$	k, l	l	h	$Ia\bar{3}$	206				

Table 1.6.4.28
Reflection conditions and possible space groups with Bravais lattice *cI* and Laue class $m\bar{3}m$; *hkl* are permutable; Patterson symmetry $Im\bar{3}m$

Reflection conditions				Space group	No.	Space group	No.	Space group	No.
hkl	$0kl$	$h \pm h\,l$	$h00$						
$h + k + l$	$k + l$	l	h	***I*432**	211	$I\bar{4}3m$	217	$Im\bar{3}m$	229
$h + k + l$	$k + l$	l	$h = 4n$	***I*4$_1$32**	214				
$h + k + l$	$k + l$	$2h + l = 4n$	$h = 4n$	$I\bar{4}3d$	220				
$h + k + l$	k, l	$2h + l = 4n$	$h = 4n$	$Ia\bar{3}d$	230				

Table 1.6.4.29
Reflection conditions and possible space groups with Bravais lattice *cF* and Laue class $m\bar{3}$; *hkl* are cyclically permutable; Patterson symmetry $Fm\bar{3}$

Reflection conditions				Space group	No.	Space group	No.
hkl	$0kl$	$h \pm h\,l$	$h00$				
$h + k, h + l, k + l$	k, l	$h + l$	h	***F*23**	196	$Fm\bar{3}$	202
$h + k, h + l, k + l$	$k + l = 4n; k, l$	$h + l$	$h = 4n$	$Fd\bar{3}$	203		

Table 1.6.4.30
Reflection conditions and possible space groups with Bravais lattice *cF* and Laue class $m\bar{3}m$; *hkl* are permutable; Patterson symmetry $Fm\bar{3}m$

Reflection conditions				Space group	No.	Space group	No.	Space group	No.
hkl	0*kl*	$h \pm hl$	*h*00						
$h+k, h+l, k+l$	k, l	$h+l$	h	***F*432**	209	$F\bar{4}3m$	216	$Fm\bar{3}m$	225
$h+k, h+l, k+l$	k, l	$h+l$	$h=4n$	***F*4$_1$32**	210				
$h+k, h+l, k+l$	k, l	h, l	h	$F\bar{4}3c$	219	$Fm\bar{3}c$	226		
$h+k, h+l, k+l$	$k+l=4n; k, l$	$h+l$	$h=4n$	$Fd\bar{3}m$	227				
$h+k, h+l, k+l$	$k+l=4n; k, l$	h, l	$h=4n$	$Fd\bar{3}c$	228				

and have not yet enjoyed widespread distribution, use and acceptance by the community. Flack *et al.* (2011) and Parsons *et al.* (2012) give detailed information on these calculations.

1.6.5.1.2. Status of centrosymmetry and resonant scattering

The basic starting point in this analysis is the following linear transformation of $|F(hkl)|^2$ and $|F(\overline{hkl})|^2$, applicable to both observed and model values, to give the average (A) and difference (D) intensities:

$$A(hkl) = \tfrac{1}{2}[|F(hkl)|^2 + |F(\overline{hkl})|^2],$$
$$D(hkl) = |F(hkl)|^2 - |F(\overline{hkl})|^2.$$

In equation (1.6.2.1), $A(hkl)$ was denoted by $|F_{\rm av}(hkl)|^2$. The expression for $D(hkl)$ corresponding to that for $A(hkl)$ given in equation (1.6.2.1) and using the same nomenclature is

$$D(\mathbf{h}) = \sum_{i,j}[(f_i + f_i')f_j'' - (f_j + f_j')f_i'']\sin[2\pi\mathbf{h}(\boldsymbol{r}_i - \boldsymbol{r}_j)].$$

In general $|D(hkl)|$ is small compared to $A(hkl)$. A compound with an appreciable resonant-scattering contribution has $|D(hkl)| \approx 0.01A(hkl)$, whereas a compound with a small resonant-scattering contribution has $|D(hkl)| \approx 0.0001A(hkl)$. For centric reflections, $D_{\rm model} = 0$, and so the values of $D_{\rm obs}(hkl)$ of these are entirely due to random uncertainties and systematic errors in the intensity measurements. $D_{\rm obs}(hkl)$ of acentric reflections contains contributions both from the random uncertainties and the systematic errors of the data measurements, and from the differences between $|F(hkl)|^2$ and $|F(\overline{hkl})|^2$ which arise through the effect of resonant scattering. A slight experimental limitation is that a data set of intensities needs to contain both reflections *hkl* and $\overline{hkl}$ in order to obtain $A_{\rm obs}(hkl)$ and $D_{\rm obs}(hkl)$.

The Bijvoet ratio, defined by

$$\chi = \frac{\langle D^2\rangle^{1/2}}{\langle A\rangle},$$

is the ratio of the root-mean-square value of D to the mean value of A. In a structure analysis, two independent estimates of the Bijvoet ratio are available and their comparison leads to useful information as to whether the crystal structure is centrosymmetric or not.

The first estimate arises from considerations of intensity statistics leading to the definition of the Bijvoet ratio as a value called Friedif$_{\rm stat}$, whose functional form was derived by Flack & Shmueli (2007) and Shmueli & Flack (2009). One needs only to know the chemical composition of the compound and the wavelength of the X-radiation to calculate Friedif$_{\rm stat}$ using various available software.

The second estimate of the Bijvoet ratio, Friedif$_{\rm obs}$, is obtained from the observed diffraction intensities. One problematic point in the evaluation of Friedif$_{\rm obs}$ arises because A and D do not have the same dependence on $\sin\theta/\lambda$ and it is necessary to eliminate this difference as far as possible. A second problematic point in the calculation is to make sure that only acentric reflections of any of the noncentrosymmetric point groups in the chosen Laue class are selected for the calculation of Friedif$_{\rm obs}$. In this way one is sure that if the point group of the crystal is centrosymmetric, all of the chosen reflections are centric, and if the point group of the crystal is noncentrosymmetric, all of the chosen reflections are acentric. The necessary selection is achieved by taking only those reflections that are general in the Laue group. To date (2015), the calculation of Friedif$_{\rm obs}$ is not available in distributed software. On comparison of Friedif$_{\rm stat}$ with Friedif$_{\rm obs}$, one is able to state with some confidence that:

(1) if Friedif$_{\rm obs}$ is much lower than Friedif$_{\rm stat}$, then the crystal structure is either centrosymmetric, and random uncertainties and systematic errors in the data set are minor, or noncentrosymmetric with the crystal twinned by inversion in a proportion close to 50:50;
(2) if Friedif$_{\rm obs}$ is close in value to Friedif$_{\rm stat}$, then the crystal is probably noncentrosymmetric and random uncertainties and systematic errors in the data set are minor. However, data from a centrosymmetric crystal with large random uncertainties and systematic errors may also produce this result; and
(3) if Friedif$_{\rm obs}$ is much larger than Friedif$_{\rm stat}$ then either the data set is dominated by random uncertainties and systematic errors or the chemical formula is erroneous.

Example 1

The crystal of compound Ex1 (Udupa & Krebs, 1979) is known to be centrosymmetric (space group $P2_1/c$) and has a significant resonant-scattering contribution, Friedif$_{\rm stat}$ = 498 and Friedif$_{\rm obs}$ = 164. The comparison of Friedif$_{\rm stat}$ and Friedif$_{\rm obs}$ indicates that the crystal structure is centrosymmetric.

Example 2

The crystal of compound Ex2, potassium hydrogen (2*R*,3*R*) tartrate, is known to be enantiomerically pure and appears in space group $P2_12_12_1$. The value of Friedif$_{\rm obs}$ is 217 compared to a Friedif$_{\rm stat}$ value of 174. The agreement is good and allows the deduction that the crystal is neither centrosymmetric, nor twinned by inversion in a proportion near to 50:50, nor that the

Table 1.6.5.1
R_{merge} values for Ex2 for the 589 sets of general reflections of *mmm* which have all eight measurements in the set

R_{merge} (%)	*mmm*	2*mm*	*m*2*m*	*mm*2	222
R_A	1.30	1.30	1.30	1.30	1.30
R_D	100.0	254.4	235.7	258.1	82.9

Table 1.6.5.2
R_{merge} values for Ex1 for the 724 sets of general reflections of 2/*m* which have all four measurements in the set

R_{merge} (%)	2/*m*	*m*	2
R_A	1.29	1.29	1.29
R_D	100.0	98.3	101.7

data set is unsatisfactorily dominated by random uncertainty and systematic error.

Example 3

The crystals of compound Ex3 (Zhu & Jiang, 2007) occur in Laue group $\overline{1}$. One finds Friedif_{stat} = 70 and Friedif_{obs} = 499. The huge discrepency between the two shows that the observed values of D are dominated by random uncertainty and systematic error.

1.6.5.1.3. Resolution of noncentrosymmetric ambiguities

It was shown in Section 1.6.5.1.2 that under certain circumstances it is possible to determine whether or not the space group of the crystal investigated is centrosymmetric. Suppose that the space group was found to be noncentrosymmetric. In each Laue class, there is one centrosymmetric point group and one or more noncentrosymmetric point groups. For example, in the Laue class *mmm* we need to distinguish between the point groups 222, 2*mm*, *m*2*m* and *mm*2, and of course between the space groups based on them. We shall show that it is possible in practice to distinguish between these noncentrosymmetric point groups using intensity differences between Friedel opposites caused by resonant scattering.

An excellent intensity data set from a crystal (Ex2 above) of potassium hydrogen (2*R*, 3*R*) tartrate, measured with a wavelength of 0.7469 Å at 100 K, was used. The Laue group was assumed to be *mmm*. The raw data set was initially merged and averaged in point group 1 and all special reflections of the Laue group *mmm* (*i.e.* 0*kl*, *h*0*l*, *hk*0, *h*00, 0*k*0, 00*l*) were set aside. The remaining data were organized into sets of reflections symmetry-equivalent under the Laue group *mmm*, and only those sets (589 in all) containing all 8 of the *mmm*-symmetry-equivalent reflections were retained. Each of these sets provides 4 A_{obs} and 4 D_{obs} values which can be used to calculate R_{merge} values appropriate to the five point groups in the Laue class *mmm*. The results are given in Table 1.6.5.1. The value of 100% for R_{merge} in a centrosymmetric point group, such as *mmm* or 2/*m*, arises by definition and not by coincidence. The R_D of the true point group has the lowest value, which is noticeably different from the other choices of point group.

The crystal of Ex1 above (space group $P2_1/c$) was treated in a similar manner. Table 1.6.5.2 shows that R_D values display no preference between the three point groups in Laue class 2/*m*.

Intensity measurements comprising a full sphere of reflections are essential to the success of the R_{merge} tests described in this section.

1.6.5.1.4. Data evaluation after structure refinement

There is an excellent way in which to evaluate both data measurement and treatment procedures, and the fit of the model to the data, including the space-group assignment, at the completion of structure refinement. This technique is applicable both to noncentrosymmetric and to centrosymmetric crystals. A scattergram of D_{obs} against D_{model}, and $2A_{obs}$ against $2A_{model}$ pairs are plotted on the same graph. All (D_{obs}, D_{model}) pairs are plotted together with those ($2A_{obs}$, $2A_{model}$) pairs which have $2A_{obs} < |D_{obs}|_{max}$. The range of values on the axes of the model and of the observed values should be identical. For acentric reflections, for both A and D, a good fit of the observed to the model quantities shows itself as a straight line of slope 1 passing through the origin, with some scatter about this ideal straight line. For an individual reflection, 2A and D are, respectively, the sum and the difference of the same quantities and they have identical standard uncertainties. It is thus natural to select 2A and D to plot on the same graph. In practice one sees that the spread of the 2A plot increases with increasing value of 2A. Fig. 1.6.5.1 shows the 2AD plot for Ex2 of Example 2 in Section 1.6.5.1.2, which is most satisfactory and confirms the choice of point group from the use of R_{merge}. The conventional R value for all reflections is 3.1% and for those shown in Fig. 1.6.5.1 it is 10.4%. The R value for all D values is good at 51.1%. Fig. 1.6.5.2 shows the 2AD plot for Ex1 of Example 1 in Section 1.6.5.1.2. The structure model is centrosymmetric so all D_{model} values are zero. The conventional R value on A for all reflections is 4.3% and for those shown in Fig. 1.6.5.2 it is 9.1%. The R value on all the D values is 100%.

1.6.5.2. Space-group determination in macromolecular crystallography

For macromolecular crystallography, succinct descriptions of space-group determination have been given by Kabsch (2010*a*,*b*, 2012) and Evans (2006, 2011). Two characteristics of macromolecular crystals give rise to variations on the small-molecule procedures described above.

The first characteristic is the large size of the unit cell of macromolecular crystals and the variation of the cell dimensions from one crystal to another. This makes the determination of the Bravais lattice by cell reduction problematic, as small changes of cell dimensions give rise to differences in the assignment. Kabsch (2010*a*,*b*, 2012) uses a 'quality index' from each of Niggli's 44 lattice characters to come to a best choice. Grosse-Kunstleve *et al.* (2004) and Sauter *et al.* (2004) have found that some commonly used methods to determine the Bravais lattice are susceptible to numerical instability, making it possible for high-symmetry Bravais lattice types to be improperly identified. Sauter *et al.* (2004, 2006) find from practical experience that a deviation δ as high as 1.4° from perfect alignment of direct and reciprocal lattice rows must be allowed to construct the highest-symmetry Bravais type consistent with the data. Evans (2006) uses a value of 3.0°. The large unit-cell size also gives rise to a large number of reflections in the asymmetric region of reciprocal space, and taken with the tendency of macromolecular crystals to decompose in the X-ray beam, full-sphere data sets are uncommon. This means that confirmation of the Laue class by means of values of R_{int} (R_{merge}) are rarer than with small-molecule crystallography, although Kabsch (2010*b*) does use a 'redundancy-independent R factor'. Evans (2006, 2011) describes methods very similar to those given as the second stage in Section 1.6.2.1. The conclusion of Sauter *et al.* (2006) and Evans (2006) is that R_{int} values as high

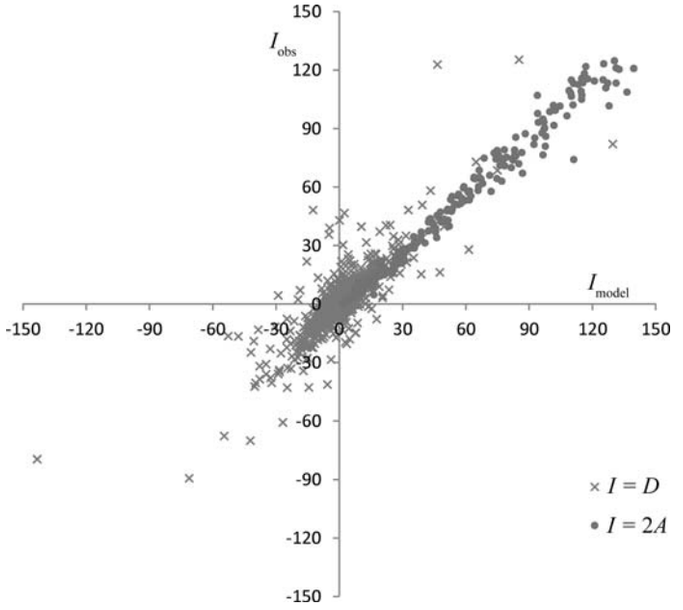

Figure 1.6.5.1
Data-evaluation plot for crystal Ex2. The plot shows a scattergram of all (D_{obs}, D_{model}) pairs and those ($2A_{obs}$, $2A_{model}$) pairs in the same intensity range as the D values.

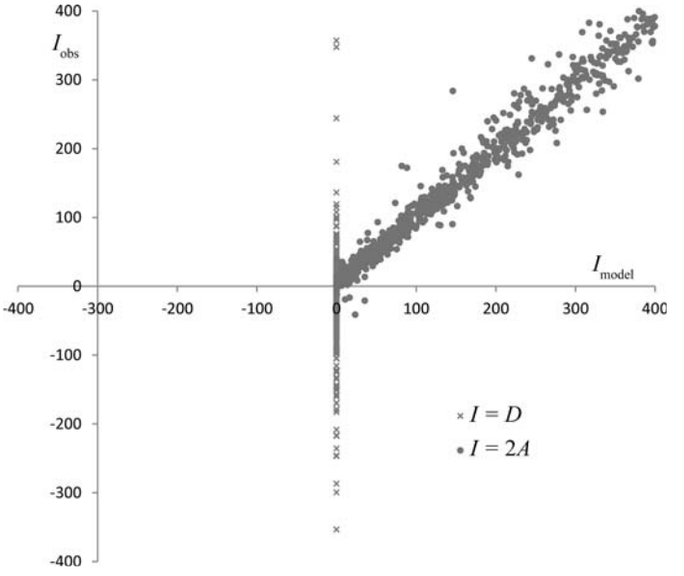

Figure 1.6.5.2
Data-evaluation plot for crystal Ex1. The plot shows a scattergram of all (D_{obs}, D_{model}) and some ($2A_{obs}$, $2A_{model}$) data points.

as 25% must be permitted in order to assemble an optimal set of operations to describe the diffraction symmetry. Another interesting procedure, accompanied by experimental proof, has been devised by Sauter *et al.* (2006). They show that it is clearer to calculate R_{merge} values individually for each potential symmetry operation of a target point group rather than comparing R_{merge} values for target point groups globally. According to Sauter *et al.* (2006) the reason for this improvement lies in the lack of intensity data relating some target symmetry operations.

The second characteristic of macromolecular crystals is that the compound is known, or presumed, to be chiral and enantiomerically pure, so that the crystal structure is chiral. This limits the choice of space group to the 65 Sohncke space groups containing only translations, pure rotations or screw rotations. For ease of use, these have been typeset in bold in Tables 1.6.4.2–1.6.4.30.

For the evaluation of protein structures, Poon *et al.* (2010) apply similar techniques to those described in Section 1.6.2.3. The major tactical objective is to identify pairs of α-helices that have been declared to be symmetry-independent in the structure solution but which may well be related by a rotational symmetry of the crystal structure. Poon *et al.* (2010) have been careful to test their methodology against generated structural data before proceeding to tests on real data. Their results indicate that some 2% of X-ray structures in the Protein Data Bank potentially fit in a higher-symmetry space group. Zwart *et al.* (2008) have studied the problems of under-assigned translational symmetry operations, suspected incorrect symmetry and twinned data with ambiguous space-group choices, and give illustrations of the uses of group–subgroup relations.

1.6.5.3. Space-group determination from powder diffraction

In powder diffraction, the reciprocal lattice is projected onto a single dimension. This projection gives rise to the major difficulty in interpreting powder-diffraction patterns. Reflections overlap each other either exactly, owing to the symmetry of the lattice metric, or approximately. This makes the extraction of the integrated intensities of individual Bragg reflections liable to error. Experimentally, the use of synchrotron radiation with its exceedingly fine and highly monochromatic beam has enabled considerable progress to be made over recent years. Other obstacles to the interpretation of powder-diffraction patterns, which occur at all stages of the analysis, are background interpretation, preferred orientation, pseudo-translational symmetry and impurity phases. These are general powder-diffraction problems and will not be treated at all in the current chapter. The reader should consult David *et al.* (2002) and David & Shankland (2008) or the forthcoming new volume of *International Tables for Crystallography* (Volume H, *Powder Diffraction*) for further information.

It goes without saying that the main use of the powder method is in structural studies of compounds for which single crystals cannot be grown.

Let us start by running through the three stages of extraction of symmetry information from the diffraction pattern described in Section 1.6.2.1 to see how they apply to powder diffraction.

(1) Stage 1 concerns the determination of the Bravais lattice from the experimentally determined cell dimensions. As such, this process is identical to that described in Section 1.6.2.1. The obstacle, arising from peak overlap, is the initial indexing of the powder pattern and the determination of a unit cell, see David *et al.* (2002) and David & Shankland (2008).

(2) Stage 2 concerns the determination of the point-group symmetry of the intensities of the Bragg reflections. As a preparation to stages 2 and 3, the integrated Bragg intensities have to be extracted from the powder-diffraction pattern by one of the commonly used profile analysis techniques [see David *et al.* (2002) and David & Shankland (2008)]. The intensities of severely overlapped reflections are subject to error. Moreover, the exact overlap of reflections owing to the symmetry of the lattice metric makes it impossible to distinguish between high- and low-symmetry Laue groups in the same family *e.g.* between 4/*m* and 4/*mmm* in the tetragonal family and $m\bar{3}$ and $m\bar{3}m$ in the cubic family. Likewise,

differences in intensity between Friedel opposites, *hkl* and $\overline{hkl}$, are hidden in a powder-diffraction pattern and the techniques of Section 1.6.5.1 are inapplicable. It is also known that experimental results on structure-factor statistics described in Section 1.6.2.2 are sensitive to the algorithm used to extract the integrated Bragg intensities from the powder-diffraction pattern. One procedure tends to produce intensity statistics typical of the noncentrosymmetric space group $P1$ and another those of the centrosymmetric space group $P\overline{1}$. In all, nothing much can be learnt from stage 2 for a powder-diffraction pattern. As a consequence, space-group determination from powder diffraction relies entirely on the Bravais lattice derived from the indexing of the diffraction pattern in stage 1 and the detection of systematic absences in stage 3.

(3) Stage 3 concerns the identification of the conditions for possible systematic absences. However, Bragg-peak overlap causes difficulties with determining systematic absences. For powder-diffraction peaks at small values of $\sin\theta/\lambda$, the problem is rarely severe, even for low-resolution laboratory powder-diffraction data. Potentially absent reflections at higher values of $\sin\theta/\lambda$ often overlap with other reflections of observable intensity. Accordingly, conclusions about the presence of space-group symmetry operations are generally drawn on the basis of a very small number of clear intensity observations. Observing lattice-centring absences is usually relatively easy. In the case of molecular organic materials, considerable help in space-group selection comes from the well known frequency distribution of space groups, where some 80% of compounds crystallize in one of the following: $P2_1/c$, $P\overline{1}$, $P2_12_12_1$, $P2_1$ and $C2/c$. Practical methods of proceeding are described by David & Sivia (2002). It should also be pointed out that Table 1.6.4.1 in this chapter may often be found to be helpful. For example, if it is known that the Bravais lattice is of type *cP*, Table 1.6.4.1 tells us that the possible Laue classes are $m\overline{3}$ and $m\overline{3}m$ and the possible space groups can be found in Tables 1.6.4.25 and 1.6.4.26, respectively. The appropriate reflection conditions are of course given in these tables. All relevant tables can thus be located with the aid of Table 1.6.4.1 if the Bravais lattice is known.

There has been considerable progress since 2000 in the automated extraction by software of the set of conditions for reflections from a powder-diffraction pattern for undertaking stage 3 above. Once the conditions have been identified, Tables 1.6.4.2–1.6.4.30 are used to identify the corresponding space groups. The output of such software consists of a ranked list of complete sets of conditions for reflections (*i.e.* the horizontal rows of conditions given in Tables 1.6.4.2–1.6.4.30). Accordingly, the best-ranked set of conditions is at the top of the list followed by others in decreasing order of appropriateness. The list thus is answering the question: Which is the most probable set of reflection conditions for the data to hand? Such software uses integrated intensities of Bragg reflections extracted from the powder pattern and, as mentioned above, the results are sensitive to the particular profile integration procedure used. Moreover, only ideal Wilson (1949) p.d.f.'s for space groups $P1$ and $P\overline{1}$ are implemented. The art of such techniques is to find appropriate criteria such that the most likely set of reflection conditions is clearly discriminated from any others. Altomare *et al.* (Altomare, Caliandro, Camalli, Cuocci, da Silva *et al.*, 2004; Altomare, Caliandro, Camalli, Cuocci, Giacovazzo *et al.*, 2004; Altomare *et al.*, 2005, 2007, 2009) have used a probabilistic approach combining the probabilities of individual symmetry operations of candidate space groups. The approach is pragmatic and has evolved over several versions of the software. Experience has accumulated through use of the procedure and the discrimination of the software has consequently improved. Markvardsen *et al.* (2001, 2012) commence with an in-depth probabilistic analysis using the concepts of Bayesian statistics which was demonstrated on a few test structures. Later, Markvardsen *et al.* (2008) made software generally available for their approach. Vallcorba *et al.* (2012) have also produced software for space-group determination, but give little information on their algorithm.

1.6.6. Space groups for nanocrystals by electron microscopy

By J. C. H. Spence

The determination of crystal space groups may be achieved by the method of convergent-beam electron microdiffraction (CBED) using a modern transmission electron microscope (TEM). A detailed description of the CBED technique is given by Tanaka (2008) in Section 2.5.3 of Volume B; here we give a brief overview of the capabilities of the method for space-group determination, for completeness. A TEM beam focused to nanometre dimensions allows study of nanocrystals, while identification of noncentrosymmetric crystals is straightforward, as a result of the strong multiple scattering normally present in electron diffraction. (Unlike single scattering, this does not impose inversion symmetry on diffraction patterns, but preserves the symmetry of the sample and its boundaries.) CBED patterns also allow direct determination of screw and glide space-group elements, which produce characteristic absences, despite the presence of multiple scattering, in certain orientations. These absences, which remain for all sample thicknesses and beam energies, may be shown to occur as a result of an elegant cancellation theorem along symmetry-related multiple-scattering paths (Gjønnes & Moodie, 1965). Using all of the above information, most of the 230 space groups can be distinguished by CBED. The remaining more difficult cases (such as space groups that differ only in the location of their symmetry elements) are discussed in Spence & Lynch (1982), Eades (1988), and Saitoh *et al.* (2001). Enantiomorphic pairs require detailed atomistic simulations based on a model, as in the case of quartz (Goodman & Secomb, 1977). Multiple scattering renders Bragg intensities sensitive to structure-factor phases in noncentrosymmetric structures, allowing these to be measured with a tenth of a degree accuracy (Zuo *et al.*, 1993). Unlike X-ray diffraction, electron diffraction is very sensitive to ionicity and bonding effects, especially at low angles, allowing extinction-free charge-density mapping with high accuracy (Zuo, 2004; Zuo *et al.*, 1999). Because of its sensitivity to strain, CBED may also be used to map out local phase transformations which cause space-group changes on the nanoscale (Zuo, 1993; Zhang *et al.*, 2006).

In simplest terms, a CBED pattern is formed by enlarging the incident beam divergence in the transmission diffraction geometry, as first demonstrated G. Mollenstedt in 1937 (Kossel & Mollenstedt, 1942). Bragg spots are then enlarged into discs, and the intensity variation within these discs is studied, in addition to that of the entire pattern, in the CBED method. The intensity variation within a disc displays a complete rocking curve in each of the many diffracted orders, which are simultaneously excited